DOI 10.1007/s11595-012-0574-4

Flame Retardancy, Smoke Suppression Effect and Mechanism of Aryl Phosphates in Combination with Magnesium Hydroxide in Polyamide 6

CHEN Jun[1], LIU Shumei[1,2,*], JIANG Zhijie[1], ZHAO Jianqing[1]

(1. College of Materials Science and Engineering, South China University of Technology, Guangzhou 510640, China; 2. The Key Lab of GD for High Property and Functional Macromolecular Materials, South China University of Technology, Guangzhou 510640, China)

Abstract: The flammability, smoke emission behavior and mechanical properties of two oligomeric aryl phosphates [bisphenol A bis(diphenyl phosphate) (BDP) and resorcinol bis(diphenyl phosphate) (RDP)] combined with magnesium hydroxide (MH) in polyamide 6 (PA6) have been investigated. Combining 5 wt% BDP, 50 wt% MH imparts a limiting oxygen index (LOI) of 40.9% and UL94 V-0 rating to PA6, meanwhile the peak rate of smoke release (pRSR), total release of smoke (TSR) and Izod notched impact strength are 41%, 33% and 233% relative to the corresponding value of 55 wt% MH without BDP, respectively. Dynamic mechanical analysis (DMA) indicates that the improvement of toughness attributes to the enhanced compatibility between MH and PA6 by adding BDP. Furthermore, based on the comprehensive analysis of thermogravimetry (TG), cone calorimeter and SEM-EDX investigations, possible flame retardancy and smoke suppression mechanisms were revealed. Besides the fuel dilution and barrier effect of MH, the combination of MH and RDP shows an additional flame inhibition effect. The combination of MH and BDP results in a dominant condensed phase barrier effect which leads to obvious reduction on smoke emission and flammability.

Key words: flame retardancy; smoke suppression; oligomeric aryl phosphate; magnesium hydroxide; polyamide 6

1 Introduction

Polyamide 6 (PA6) is widely used in electronic and electrical industry because of its excellent mechanical and electrical properties. However, PA6 is a combustible material which burns with flammable dripping and poisonous smoke releasing. As smoke is a major cause of death in fires, it is essential for flame retardants to keep smoke production to a minimum in order to reduce the overall fire hazard. Unfortunately the traditionally main flame retardants are halogen compounds, including bromine and chlorine compounds, which decrease the flammability of PA6 but release more toxic gases and corrosive smoke on combustion[1]. Nowadays advanced halogen-free and low smoke flame retarded systems are one of the most popular topics of relevant polymer materials research and development. The possible effective solutions have been found for metal hydroxides and phosphorus compounds[2-5].

Organic or inorganic phosphorus compounds are the most common flame retardants as halogen-free alternative. As described in literatures[5-8], phosphorus-based flame retardants could act in both condensed and gas phase. The gas phase action of phosphorus results from flame inhibition through radical trapping reaction, which increases toxic smoke production. Hence, most commercialized phosphorus-based flame retardants, such as red phosphorus (RP) and phosphinates, also have the same disadvantage that increase the smoke production on combustion, although a little lower than halogen compounds[9,10]. Oligomeric aryl phosphates like resorcinol bis(diphenyl phosphate) (RDP) and bisphenol A bis(diphenyl phosphate) (BDP), have been found application as flame retardants and plasticizers in a range of plastics. It was proposed that RDP shows some and BDP a crucial condensed phase action in polycarbonate alloy[11]. These properties of oligomeric aryl phosphates might favor the smoke suppression.

(Received: Oct. 6, 2011; Accepted: Mar. 8, 2012)

CHEN Jun (陈俊): Ph D; E-mail:augustus.chen@hotmail.com

*Corresponding author: LIU Shumei(刘述梅): Assoc. Prof.; Ph D; E-mail: liusm@scut.edu.cn

Funded by Chinese 973 National Key Scientific Project (No. 2011CB606002), Key Project in Science and Technology of Guangdong Province (No. 2010B010800018) and the Cultivation Fund of the Key Scientific and Technical Innovation Project, Department of Education of Guangdong Province (No. cxzd1008)

Metal hydroxides, typically alumina trihydrate (ATH) and magnesium hydroxide (MH), are fillers and extensively used as halogen-free flame retardants which have endothermic decomposition accompanied by the release of water, resulting in cooling and dilution effect to inhibit flame[1,5,12]. Although essentially non-toxic and reduction of toxic smoke are the major advantages of metal hydroxides, high loadings to achieve adequate flame retardancy often lead to processing difficulties and marked deterioration in other critical characteristics, including mechanical and electrical properties. The combination of metal hydroxides with other high-effective flame retardants is considered as an approach suitable for commercial utilization.

MH can act as flame retardants and excellent smoke suppressants; moreover oligomeric aryl phosphates favor smoke suppression. Hence the synergistic effects between them in flame retardancy and smoke suppression were the focus of this work. The flame retardancy, mechanical properties and smoke suppression effects of PA6 flame-retarded by the combinations of MH with oligomeric aryl phosphates were investigated. Further, the influences of oligomeric aryl phosphates on flame retardancy mechanisms were discussed.

2 Experimental

A series of different PA6 materials with certain proportion of MH and two varied oligomeric aryl phosphates were investigated. PA6 (M32800, Meida-DSM) mixed with MH (Magnifin H-5 IV, Albemarle), RDP (Fyrolflex RDP, ICL-IP) and BDP (Fyrolflex BDP, ICL-IP) following the proportion of Table 1 in a high-speed mixer (SHR-25A, Zhangjiagang Yili Machinery Factory, China). These mixtures were melt-kneaded and granulated on a 26 mm twin-screw extruder (LTE26/40, Labtech, Germany) at a temperature of 215-230 ℃ and a screw speed of 150 $r \cdot min^{-1}$. The obtained pellets were dried in vacuum at the temperature of 80 ℃ to constant mass. Then they were injection molded (injector: P50E, Hongli Machinery Company, China) at an injection temperature of 220-240 ℃ into various shapes, sizes and forms of different test specimens.

The flammability of the samples was determined by limiting oxygen index (LOI) according to ISO 4589:1999 (specimen size: 150 mm×10 mm×4 mm) on an oxygen index instrument (FTT0077, FTT, UK) and by using the standard UL 94-2009 vertical tests (specimen size: 120 mm×12.7 mm×3.2 mm) on a UL94 flame chamber (FTT0082, FTT, UK).

The mechanical properties of materials were tested. Tensile strength and flexural modulus were tested by a universal material tester (BT1-FR010TH A50, Zwick, Germany), following ISO 527:1996 (tensile strength) and ISO 178:2003 (flexural modulus). The Izod notched impact strength was tested by a pendulum impact tester (5113, Zwick, Germany) following ISO 180:2001.

A TG209 F1 (Netzsch, Germany) thermogravimentry (TG) apparatus was used to investigate the thermal decomposition. All measurements were performed under nitrogen at a heating rate of 20 ℃min^{-1}. The sample weight was about 10 mg. Values for residues were taken at 800 ℃. The standard deviation of the TG results was about 1 wt% (including the contribution of buoyancy forces).

Dynamic mechanical analysis (DMA) was performed on a DMA apparatus (DMA-242C, Netzsch, Germany) operating in tensile mode at a frequency of 10 Hz in the temperature range of -80 ℃ to 140 ℃ with a heat rate of 10 °Cmin^{-1}.

To characterize the forced-flaming and smoke emission behavior a cone calorimeter (FTT0007, FTT, UK) was used, following ISO 5660:2002, with external heat fluxes of 50 kWm^{-2}. All samples (specimen size: 100 mm×100 mm×6 mm) were measured in a horizontal position using a retainer frame to reduce unrepresentative edge-burning. The decreased sample area was taken into account for the calculations. The flame-out was defined as the end of test. And all measurements were repeated thrice. Residue analysis was performed by scanning electron microscopy (SEM) (Nova NanoSEM 430, FEI, Netherland) and energy dispersive X-ray spectroscopy (EDX) (INCA350, Oxford, UK).

3 Results and discussion

3.1 Flammability and mechanical properties

To evaluate the flammability of PA6 and the flame retarded PA6, LOI and UL94 vertical tests were conducted, while corresponding tensile strength, Izod notched impact strength and flexural modulus tests were used to investigate the mechanical properties of samples. The results and the composition of samples are summarized in Table 1. Even though the MH content is up to 55 wt% in sample $2^{\#}$ and resulted in a disastrous deterioration in the toughness of material (Izod notched impact strength decreased to only 53% of

Table 1 Composition, flammability and mechanical properties of materials

Sample	Composition				LOI /%	UL 94 rating	Izod notched impact strength /kJ • m^{-2}	Tensile strength /MPa	Flexural modulus /GPa
	PA6 /wt%	MH /wt%	RDP /wt%	BDP /wt%					
1#	100	0	0	0	22.5	NB	7.3	60.0	2.0
2#	45	55	0	0	40.5	V-1	3.9	83.2	6.4
3#	45	50	5	0	47.0	V-0	6.2	66.2	2.7
4#	45	50	0	5	40.9	V-0	9.1	50.2	2.2

sample 1#), sample 2# only achieved V-1 classification in UL94 vertical test and the LOI value increased to 40.5%. The flame retardancy efficiency of using MH alone was unsatisfied in PA6.

The MH content could be reduced to 50 wt% in the presence of 5 wt% oligomeric aryl phosphates while their flame retardancy achieved UL94 V-0 rating. Compared to sample 2#, with 5 wt% RDP instead of 5 wt% MH, the LOI value of sample 3# increased from 40.5% to 47.0%, and Izod notched impact strength increased from 3.9 kJ•m^{-2} to 6.2 kJ•m^{-2}. Its tensile strength and flexural modulus were lower than the corresponding values of sample 2#, but still higher than pure PA6. Substituting BDP for RDP in sample 4# resulted in a further increase of Izod notched impact strength to 9.1 kJ•m^{-2}, which was even better than pure PA6. Besides, the tensile strength and flexural modulus of sample 4# were 83.7% and 110.0% of the values of pure PA6, respectively, and the LOI value was 40.9% which was slightly higher than sample 2#. The above results indicate that two kind oligomeric aryl phosphates combining with MH respectively in PA6 can concurrently enhance flame retardancy and mechanical properties. These also indicate that BDP performs better than RDP in improving the toughness of material.

3.2 Smoke emission behavior

The rate of smoke release (RSR) and total smoke release (TSR) of cone calorimeter tests was used to quantify the emission of smoke. The RSR and TSR curves of all samples are shown in Fig.1. For sample 1#, the RSR was characterized by an increasing value with time after ignition, and then a sharp RSR peak appeared at the end of the curve, with a peak value of RSR (pRSR) as high as 7.8 m^{2}s^{-1}m^{-2}. The TSR of sample 1# increased very fast, and the value at the end of combustion was 1 710 m^{2}m^{-2}. Similar smoke emission behavior was described in the literature for pure PA6[13]. The presence of MH in PA6 significantly changed the smoke emission behavior. There were two peaks at 300 s and 720 s on the RSR curve of sample 2# with the corresponding peak values of 1.7 m^{2}s^{-1}m^{-2} and 2.1 m^{2}s^{-1}m^{-2}, respectively. Besides the reducing in pRSR, the TSR of the whole burning process also decreased to 1 311 m^{2}m^{-2}.

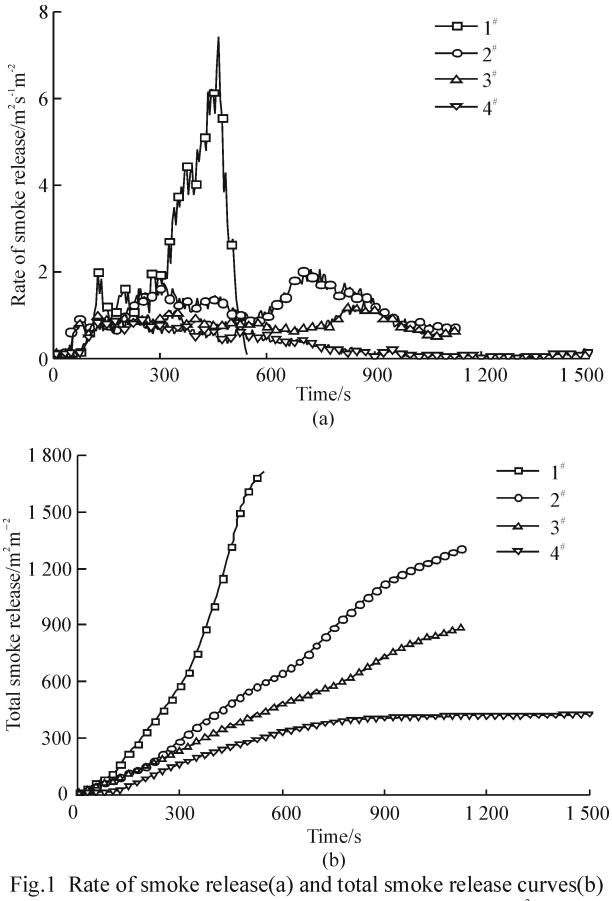

Fig.1 Rate of smoke release(a) and total smoke release curves(b) of all samples at an external heat flux of 50 kWm^{-2}

In sample 3#, the principle shape of the RSR curve was similar to sample 2#, except the second and also higher peak appeared at 870 s that was later than sample 2#. The pRSR was 1.32 m^{2}s^{-1}m^{-2}, which corresponded to a reduction of 37% compared to sample 2#. And the TSR of whole process was 885 m^{2}m^{-2}, which was reduced compared to sample 2# in the very similar order of 33%. That means the presence of RDP does not change the smoke emission behavior, but reduced the smoke release amount. With BDP adding the best smoke suppression performance was obtained, the smoke release was reduced further. Its smoke emission behavior was obviously different

to other three samples. Following a very short initial increase to the pRSR, the RSR curve of sample 4# showed a steady decrease in the whole process. The pRSR decreased to 0.8 $m^2s^{-1}m^{-2}$ at 140 s. The TSR of sample 4# was only 428 m^2m^{-2} which was less than half of sample 3#. The above results indicate that the combination of BDP and MH in PA6 performs better smoke suppression effect than MH with or without RDP.

3.3 Dynamic mechanical analysis

Fig.2 shows the variation of loss tangent (tan δ) of all four samples with temperature in DMA investigations. On the tan δ curves, two transition processes showed as two peaks, and were named as α and β, respectively. The α transition is usually related to the segment movements in non-crystalline area, so the glass transition of polymer matrix can be determined by α transition. The β transition reflects the co-moving of amido and methane[14].

When only MH was added, the α transition peak area and value were significantly decreased compared to pure PA6. No β transition peak appeared on the tan δ curve of sample 2#. The tanδ behavior of sample 2# reflected the incompatibility of MH particles with PA6 matrix[15]. In the combination of RDP and MH, the α transition peak shift to a temperature about 10 ℃ lower compared to pure PA6, the α transition peak area and value were clearly increased. But the tan δ value of β transition for sample 3# was still lower than pure PA6. The results indicated that RDP mainly acted as a plasticizer and did not enhance the compatibility between MH particles and PA6[15, 16]. When BDP and MH were combined, the α transition peak area was similar with sample 3#, its peak value was further increased. Moreover, the tan δ value of β transition for sample 4# was much higher than that of pure PA6. The tan δ behavior of sample 4# proved again that BDP enhanced the compatibility between MH particles and PA6 matrix[15, 16].

DMA results revealed the reasons of the influence of RDP and BDP on the mechanical properties. RDP only acts as a plasticizer but does not improve the compatibility. BDP also has plasticization action, but more importantly it obviously enhances the compatibility between MH particles and polymer matrix. The enhancement on compatibility not only increased the toughness of material, but also might increase the flame retardancy efficiency of MH.

3.4 Thermal decomposition behavior

In order to investigate the flame retardancy and smoke suppression mechanisms, thermal decomposition behaviors of all four samples were performed using TG apparatus. The TG results are summarized in Table 2;

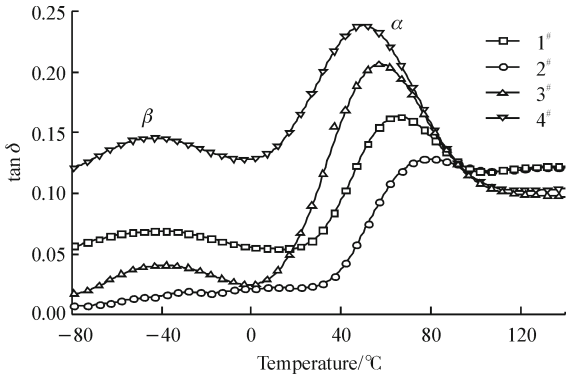

Fig.2 Loss tangent curves *versus* temperature for all samples at a test frequency 10 Hz

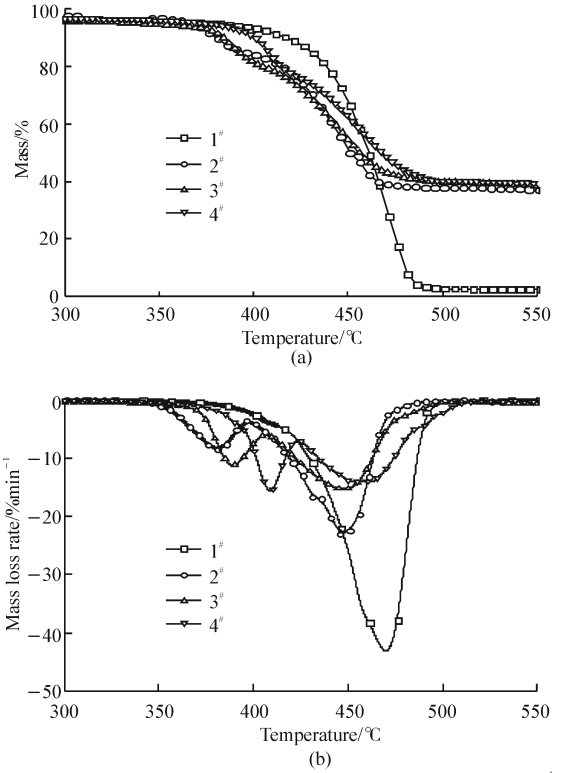

Fig.3 TG(a) and DTG(b) curves of all samples(heating rate 20 ℃ min^{-1})

both the corresponding mass and mass loss rate curves are shown in Fig.3. The thermal decomposition of sample 1# was characterized by a single decomposition step with maximum mass loss rate at 469 ℃. The resulting residue was of about 1.2 wt%. These results were in agreement with the decomposition behavior of pure PA6 in literatures[13, 17, 18].

When MH was added, the decomposition behavior changed significantly. Sample 2# decomposed in two main steps, which were respectively named as Step I and Step II on Table 2. The Step I was related to the decomposition of MH, whereas the Step II was

Table 2 Thermal analysis of all samples(based on TG investigations, heating rate 20 ℃ · min^{-1})

Sample	Step Ⅰ			Step Ⅱ			Residue at 800 ℃ /wt%
	△mass/wt%	T_{max1}[a]/℃	△T/℃	△mass/wt%	T_{max2}[b]/℃	△T/℃	
1#				96.9	469	377-497	2.5
2#	16.0	381	337-397	45.9	448	397-478	37.6
3#	19.6	389	362-407	40.4	448	407-487	38.5
4#	24.1	408	369-426	35.7	459	426-511	39.6

[a] Temperature of the maximum mass loss rate in Step Ⅰ; [b] Temperature of the maximum mass loss rate in Step Ⅱ for sample 2-4#, and temperature of the maximum mass loss rate in whole process for sample 1#.

due to the decomposition of PA6[19, 20]. The lowering of PA6 decomposition temperature (T_{max2} from 469 ℃ to 448 ℃) can be attributed to the water released by MH decomposition resulted in an additional hydrolysis process of parts of PA6[1, 5, 21].The residue at the end of test was 37.6 wt% and hence mainly consisted of MgO. Similar results were reported in the literature for MH formulations in different kinds of polyamides[19, 20].

When RDP and MH were combined in sample 3#, the Step I was shifted to a temperature about 10 ℃ higher than sample 2#, and the T_{max1} was 389 ℃. The Step II remained unaffected at 448 ℃. The stable residue at 800 ℃ was increased slightly to 38.5 wt%. The combination of BDP and MH in PA6 resulted in that the Step I of sample 4# was clearly increased about 30 ℃ compared to sample 2# with a T_{max1} at 408 ℃. Furthermore, the Step II was also shifted to a temperature about 10 ℃ higher than sample 2# and 3# with T_{max2} at 459 ℃. The increase of T_{max2} indicated that BDP effectively inhibited hydrolysis of PA6 in Step II. Compared to sample 2#, the residue at the end of TG experiment was increased by 2.0 wt% to 39.6 wt%. Considering the very low loading of BDP (only 5 wt%), adding BDP resulted in considerable increasing char formation in condensed phase.

In conclusion, combining MH and BDP enhances the thermal stability of polymer matrix in comparison with using MH only or combining MH and RDP; BDP also shows more condensed phase action than RDP. The reason could be attributed to that BDP induced a more stable and effective condensed phase cross-linking network than RDP[11, 19].

3.5 Fire behavior

The heat release rate (HRR) and total heat release (THR) curves from cone calorimeter tests using external heat fluxes of 50 kWm^{-2} are illustrated in Fig.4 and the detail cone calorimeter results are summarized in Table 3. For sample 1#, the HRR curve was characterized by a sharp peak, and the peak value of HRR (pHRR) was 718 kWm^{-2}, which is a characteristic HRR behavior of pure PA6[13, 23]. The THR at the end of test was 227.4 MJm^{-2} corresponding to values in literature[23]. With MH adding, the pHRR of sample 2# was reduced by 62% to value of 270 kWm^{-2}. An additional small peak occurred on the HRR curve of sample 2#, with the peak value of 169 kWm^{-2} at 697 s. The second HRR peak could be attributed to the protection failure of MgO surface layer under prolonged high temperature [24, 25]. The THR was reduced by 34% to value of 150.6 MJm^{-2}. The residue weight of sample 2# was 38.2 wt%, which fits well to the calculated MgO amount of 37.9 wt%. When RDP and MH were combined in PA6, the principle shape of HRR curve was similar to sample 2#. The second HRR peak was occurred at 830 s with the peak value of 170 kWm^{-2}. The pHRR was slightly reduced to 244 kWm^{-2}. The THR was slightly

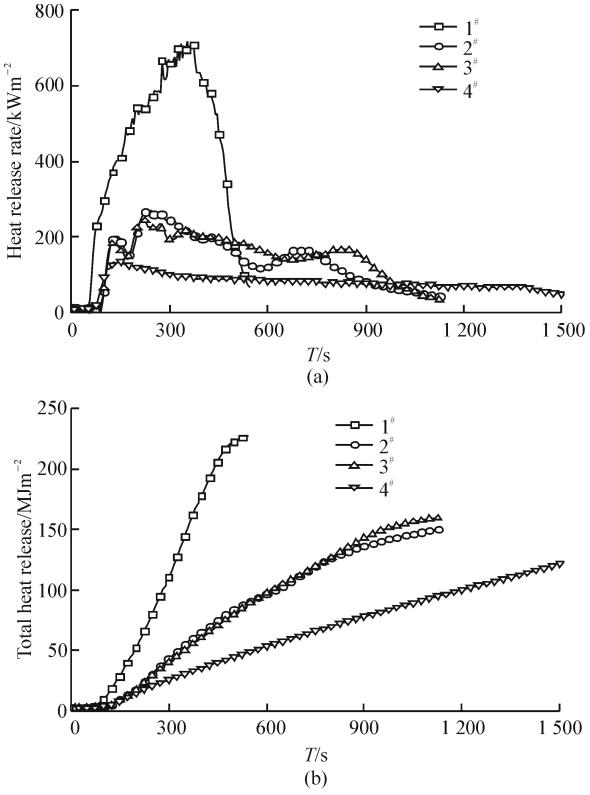

Fig.4 Heat release rate(a) and total heat release curves(b) of all samples at an external heat flux of 50 kWm^{-2}

increased to 159.5 MJm^{-2}. The residue of sample 3# was 36.9 wt%, which was only 2.4 wt% higher than its calculated MgO amount (34.5 wt%). For sample 3#, the principle shape of HRR curve indicated that the main flame retarancy effect still resulted from gas phase action. The change in pHRR, second HRR peak and residue content declared that RDP provided an additional protection for residue layer and improved the stability of residue[10, 25].

With the combination of BDP and MH a different cone calorimeter performance was obtained. On the HRR curve of sample 4#, after an initial increase in HRR during the formation of barrier layer, the HRR showed a steady decrease. The pHRR was clearly reduced to 135 kWm^{-2}, and THR also was only 121.9 MJm^{-2}. The residue was increased to 39.8 wt%, which was 5.4 wt% higher than the calculated MgO amount (34.5 wt%). These HRR behaviors were typical for a char-forming flame retardancy mechanism in condensed phase[10].

Table 3 Cone calorimeter data

Sample	THR /MJm^{-2}	pHRR /kWm^{-2}	THR/TML /($MJm^{-2}g^{-1}$)	Residue /wt%
1#	227.4	718	3.64	6.7
2#	150.6	270	2.65	38.2
3#	159.5	244	2.78	36.9
4#	121.9	135	3.02	39.8

For the analysis of the flame retardancy mechanism, the effective heat of combustion, expressed through the total heat release/total mass loss (THR/TML), was determined in Table 3. According to literature[7, 26] a higher THR/TML value indicates less flame inhibition or fuel dilution action in gas phase. For sample 2#, the THR/TML value was clearly reduced compared to pure PA6. This result was in agreement with the known main flame retardancy mechanism of MH[1, 5, 12], which is based on a fuel dilution effect of water releasing in gas phase. With the addition of RDP, the THR/TML value was slightly increased compared to sample 2#, but was still much lower than pure PA6. Hence, gas phase action is still the main flame retardancy mechanism, which includes fuel dilution of water and the flame inhibition of phosphates in this cause. For sample 4# the THR/TML value was much higher than sample 2# and 3#. Therefore the gas phase action is negligible, and an efficient condensed phase action dominates the fire retardancy mechanism.

It should be noted that the complex flame retardancy behaviors in LOI and cone calorimeter also indicate different flame retardancy mechanism. In detail, sample 3# had a higher LOI value than sample 4#, but sample 4# performed better flame retardancy property in cone calorimeter investigation. The condensed phase action of phosphorus is not dependent on the external heat flux on burning, while the gas phase action is dependant on the external heat flux and decreases when high external heat fluxes were used[7, 9, 10, 26]. In this work, the external heat flux in cone calorimeter investigation was much greater than the external heat flux in LOI test. It could be concluded that the main fire retarded action of sample 3# takes place in the gas phase. Furthermore, it could be proposed that the main fire retarded action of sample 4# results from condensed phase action.

To sum up, the strong gas phase action of MH in PA6 is remained in the combination with RDP, but when combined with BDP the gas phase action is reduced clearly while condensed phase action is dominant.

3.6 Residue analysis

Generally, the chemical composition and morphology of residue are governed by the flame retardancy mechanism and have great impacts on the actual flame retardancy. The residues of sample 3# and 4# from the cone calorimeter investigation at 50 kWm^{-2} external heat flux were collected for morphology and chemical composition analysis.

After the cone calorimeter investigation, the residue of sample 3# (Fig.5(a)) was fragmentary

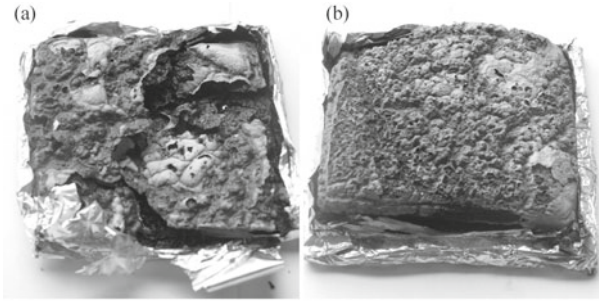

Fig. 5 Digital photos of the residues obtained in the cone calorimeter: (a)Sample 3#; (b)Sample 4#

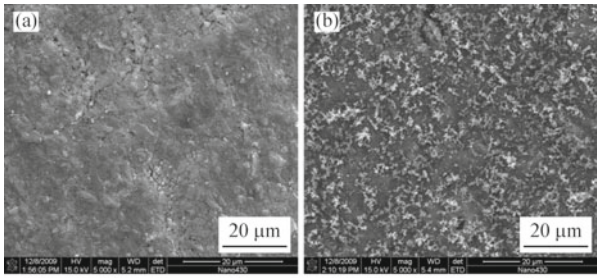

Fig.6 SEM images of the residues obtained in the cone calorimeter: (a)Sample 3#; (b)Sample 4#

and loose, and there were many huge crevasses on the surface. The residue of sample 4# (Fig.5(b)) was coherent, compact and dense. SEM images in Fig.6 show the microscopic morphology of the residue layers of the above samples. For sample 3# (Fig.6(a)), the residue layer was friable and loose, and lots of cracks and MgO particles were clearly observed on the surface of the residue. Obviously, the uncontinuous and friable residue of sample 3# is not an effective barrier layer and hardly endows the materials with enough flame retardancy, so gas phase action provides important role in this sample. By contrast, the residue of sample 4# (Fig.6(b)) showed a dense and continuous vitreous char layer, and almost no crack and MgO particle exposed on the surface. This glassy char causes a strong barrier effect against heat and volatiles diffusion. Furthermore, large number of globular char, whose diameter was about 150 nm and grouped into some short chains, was observed on the surface of the residue. These globular char results from the char formation on the surface wherein BDP acts like acid precursor[8, 11].

Table 4 Chemical composition of the residues collaged from the cone calorimeter, based on SEM–EDX analyses

Sample		Chemical composition/wt%				
		C	N	O	P	Mg
3#	Surface	14.8	1.4	54.9	0.8	28.1
	Inside	30.5	1.9	42.6	0.9	24.1
4#	Surface	34.5	1.2	43.0	0.7	20.6
	Inside	37.9	2.4	35.0	0.8	23.9

The excellent charring action of BDP during combustion was also proved by the results of EDX (Table 4). The surface and inside chemical compositions of residue of sample 3# were quite different. The carbon content of the surface was much lower than the inside of residue. This indicated that only a few organic remained on the surface of residue, thus no effective barrier layer was produced in sample 3# during combustion. The residue of sample 4# was almost homogeneous in chemical composition measured by EDX. The carbon contents on surface and inside were quite similar, and higher than the carbon content on the inside of sample 3# residue. This homogeneous composition indicated the stable organic structure in the whole residue which resulted in a strong barrier effect against flame.

4 Conclusions

The smoke emission of PA6 is obviously reduced by using MH only, but the toughness and flammability are unsatisfactory. The combination of MH and RDP in PA6 results in simultaneous improvement on flame retardancy, smoke suppression and toughness as compared to using MH only. The combination of MH and BDP improves the smoke suppression effect and toughness further. When 5 wt% BDP and 50 wt% MH were combined in PA6, the flammability gained UL94 V-0 and a LOI of 40.9%, meanwhile the pRSR, TSR and Izod notched impact strength were 41%, 33% and 233% of the corresponding value of the sample using MH alone, respectively. Its Izod notched impact strength was 124% of the value of pure PA6.

The influences of the combination of MH and RDP on mechanical properties are mainly ascribable to the plasticization effect of RDP. The compatibility of MH particles in PA6 matrix is substantially increased in combination with BDP, which results in obvious enhancement of toughness.

Adding MH in PA6 as a flame retardant and a smoke suppressant is mainly based on fuel dilution effect and MgO barrier effect. The combination of MH and RDP only engenders an additional flame inhibition effect of phosphate in gas phase. Hence, the gas phase action including the fuel dilution of MH decomposition products and flame inhibition of phosphate dominates the flame retardancy mechanism. The smoke suppression mechanism is still mainly based on fuel dilution, and the slight reduction of smoke emission is attributed to that the enhanced flame retardancy effect offers an additional protection for the residue barrier layer. The combination of MH and BDP alters the flame retardancy and smoke suppression mechanisms. The strong condensed phase action, which leads to an effective phosphorus-containing barrier layer on combustion, dominates the fire protection. The crucial condensed phase action results in the clearly reduction of smoke emission.

References

[1] J Troitzsch. *Plastics Flammability Handbook, 2nd Ed*[M]. Munchen: Hanser, 1990

[2] SY Lu, I Hamerton. Recent Developments in the Chemistry of Halogen-free Flame Retardant Polymers[J]. *Prog. Polym. Sci.,* 2002, 27(8): 1 661-1 712

[3] S V Levchik, D A Bright, G R Alessio, *et al.* New Halogen-free Fire Retardant for Engineering Plastic Applications[J]. *J. Vinyl. Addit. Technol*., 2001, 7:98-103

[4] E D Weil, S V Levchik. Current Practice and Recent Commercial

Developments in Flame Retardancy of Polyamides[J]. *J. Fire Sci.,* 2004, 22:251-264

[5] F Laoutid, L Bonnaud, M Alexandre. New Prospects in Flame Retardant Polymer Materials: From Fundamentals to Nanocomposites[J]. *Materials Sci. and Eng., R*, 2009, 63:100-125

[6] J W Lyons. Mechanisms of Fire Retardation with Phosphorus Compounds: Some Speculations[J]. *J.Fire Flammability,* 1970, 1:302-315

[7] U Braun, A I Balabanovich, B Schartel, *et al.* Influence of the Oxidation State of Phosphorus on the Decomposition and Fire Behaviour of Flame-retarded Epoxy Resin Composites[J]. *Polymer,* 2006, 47:8 495-8 508

[8] M Lewin, E D Weil. Mechanism and Modes of Action in Flame Retardancy of Polymers. In: Horrocks A R, Price D Editors. *Fire Retardant Materials*[M]. Cambridge: Woodhead Publishing, 2001

[9] B Schartel, R Kunze, D Neubert. Red Phosphorus-controlled Decomposition for Fire Retardant PA 66[J]. *J. Appl. Polym. Sci.,* 2002, 83(10):2 060-2 071

[10] U Braun, B Schartel, M A Fichera., *et al.* Flame Retardancy Mechanisms of Aluminium Phosphinate in Combination with Melamine Polyphosphate and Zinc Borate in Glass-fibre Reinforced Polyamide 6,6[J]. *Polym. Degrad. and Stab.,* 2007, 92(8):1 528-1 545

[11] K H Pawlowski, B Schartel. Flame Retardancy Mechanisms of Triphenyl Phosphate, Resorcinol Bis(Diphenyl Phosphate) and Bisphenol A Bis(Diphenyl Phosphate) in Polycarbonate/Acrylonitrile-Butadiene-Styrene Blends[J]. *Polym. Int*., 2007, 56:1 404-1 414

[12] P R Hornsby, C L Watson. A Study of the Mechanism of Flame Retardance and Smoke Suppression in Polymers Filled with Magnesium Hydroxide[J]. *Polym. Degrad. and Stab*., 1990,30(1):73-87

[13] D C O Marney, L J Russell, D Y Wu, *et al.* The Suitability of Halloysite Nanotubes as a Fire Retardant for Nylon 6[J]. *Polym. Degrad. and Stab.,* 2009, 93(10):1 971-1 984

[14] W H Li, D Y Yan. Synthesis and Characterization of Nylons Based on Hexadecane Diacid[J]. *J. Appl. Polym. Sci.,* 2003;88(10):2 462-2 467

[15] K C Manikandan-Nair, S Thomas, G Groeninckx. Thermal and Dynamic Mechanical Analysis of Polystyrene Composites Reinforced with Short Sisal Fibres[J]. *Composites Sci. and Tech.,* 2001, 61:2 519-2 529

[16] M Xie, Z G Zhang, Y Z Gu. A New Method to Characterize the Cure State of Epoxy Prepreg by Dynamic Mechanical Analysis[J]. *Thermochimica Acta,* 2009, 487:8-17

[17] P Straka, J Náhunková, Z Broová. Kinetics of Copyrolysis of Coal with Polyamide 6[J]. *Journal of Analytical and Applied Pyrolysis,* 2004, 71(1):213-221

[18] K P Pramoda, T X Liu, Z H Liu, *et al.* Thermal Degradation Behavior of Polyamide 6/Clay Nanocomposites[J]. *Polym. Degrad. and Stab.,* 2003, 81(1):47-56

[19] P R Hornsby, J Wang, R Rothon. Thermal Decomposition Behaviour of Polyamide Fire-Retardant Compositions Containing Magnesium Hydroxide Filler[J]. *Polym. Degrad. and Stab.,* 1996, 51(3):235-249

[20] G X Fei, Y Liu, Q Wang. Synergistic Effects of Novolac-based Char Former with Magnesium Hydroxide in Flame Retardant Polyamide-6[J]. *Polym. Degrad. and Stab.,* 2008, 93(7):1 351-1 356

[21] R Martens, H Gentsch, F Freund. Hydrogen Release During the Thermal Decomposition of Magnesium Hydroxide to Magnesium Oxide[J]. *Journal of Catalysis,* 1976, 44(3):366-372

[22] K H Pawlowski, B Schartel. Flame Retardancy Mechanisms of Aryl Phosphates in Combination with Boehmite in Bisphenol A Polycarbonate/Acrylonitrile-Butadiene-Styrene Blends[J]. *Polym. Degrad. and Stab.,* 2008, 93(1):657-667

[23] S Bourbigot, S Duquesne, C Jama. Polymer Nanocomposites: How to Reach Low Flammability[J]? *Macromolecular Symposia,* 2006(133):180-190

[24] A Genovese, R A Shanks. Structural and Thermal Interpretation of the Synergy and Interactions Between the Fire Retardants Magnesium Hydroxide and Zinc Borate[J]. *Polym. Degrad. and Stab.,* 2007, 92(1):2-13

[25] Z Z Li, B J Qu. Flammability Characterization and Synergistic Effects of Expandable Graphite with Magnesium Hydroxide in Halogen-free Flame-retardant EVA Blends[J]. *Polym. Degrad. and Stab.,* 2003, 81(3):401-408

[26] B Schartel, U Braun. Fire Retardancy Mechanisms of Phosphorus in Thermoplastics[J]. *Polym. Mater. Sci. Eng.,* 2004(91):152-153